

## Supporting Information

### **The role of Al<sup>3+</sup>-based aqueous electrolytes in the charge storage mechanism of MnO<sub>x</sub> cathodes**

*Véronique Balland,<sup>\*</sup> Mickaël Mateos, Arvinder Singh, Kenneth D. Harris, Christel Laberty-Robert, Benoît Limoges<sup>\*</sup>*

- I. Experimental Section
- II. Supplementary Figures
- III. Supplementary Tables
- IV. References

## I. Experimental Section

**Chemicals.** Acetic acid (Reagent plus, > 99%), KOH, HCl (Normapur, 37%), KCl (GR for analysis), ethanol absolute (EMSURE),  $\text{ZnCl}_2$  (> 98%),  $\text{Zn}(\text{CF}_3\text{SO}_3)_2$  (98%),  $\text{MnSO}_4$  monohydrate (> 99%) were purchased from Sigma-Aldrich/Merck.  $\text{Al}(\text{CF}_3\text{SO}_3)_3$  (99%) was purchased from Acros Organics. Anhydrous  $\text{AlCl}_3$  (> 99%) was purchased from Fluka.  $\text{MnCl}_2$  tetrahydrate (99%) was purchased from Alfa Aesar. Acetone (Normapur) and chloroform (Normapur) were purchased from VWR Chemicals.

**GLAD-ITO Mesoporous Electrodes.** Porous ITO thin films were prepared by the glancing angle deposition (GLAD) method followed by thermal treatment as previously described.<sup>[1]</sup> Briefly, nanostructured ITO films were deposited from ITO evaporant (Cerac, 91:9  $\text{In}_2\text{O}_3/\text{SnO}_2$  99.99% pure) in an electron-beam physical vapor deposition system (Axxis, Kurt J Lesker) on ITO-coated glass substrates (8-12  $\Omega/\square$ , Delta Technologies Ltd.). Throughout the deposition, substrates were maintained at an 80° angle with respect to impinging evaporant flux, while constantly rotating as a feedback-controlled function of the deposition rate. The film thickness was 1  $\mu\text{m}$ . Following deposition, the GLAD-ITO samples were thermally annealed in a two stage process, first under air at 500 °C and subsequently under 5%  $\text{H}_2/\text{Ar}$  flow at 375 °C, to improve and stabilize the optical and electrical properties. For such deposition conditions, the film porosity was previously estimated to be 0.5 and its density to be 4  $\text{g}\cdot\text{cm}^{-3}$ .<sup>[1]</sup> Prior to the electrochemical experiments, the GLAD-ITO electrodes were cleaned by soaking them successively in chloroform, acetone, and ethanol, each time for 30 min at 50°C. After the electrodes were left to dry, a geometric area of  $0.50 \pm 0.1 \text{ cm}^2$  was delimited by depositing an insulating layer of nail polish. After cycling, GLAD-ITO electrodes were recycled by successively soaking 5 minutes in an aqueous acidic solution containing 3 %wt  $\text{H}_2\text{O}_2$  and 30 minutes in a large volume of ultrapure water.

**Preparation of the  $\text{MnO}_2$ -coated GLAD-ITO electrodes.** *Ex situ* electrodeposition of  $\text{MnO}_2$  within the 3D structure of GLAD-ITO electrodes was performed by galvanostatic electrodeposition as previously described,<sup>[2]</sup> using a standard three-electrode cell configuration and a multichannel potentiostat/galvanostat (VSP model, BioLogic instrument). Experiments were performed at room temperature, and an SCE (+0.244 V vs. NHE) and Pt-grid were used as reference and counter electrode, respectively. For electrodeposition, GLAD-ITO electrodes were placed in 7 mL of a quiescent acetate buffer (1 M, pH 5.0) containing 0.1 M  $\text{MnCl}_2$  and 0.85 M KCl. After preconditioning by cyclic voltammetry (CV) from 0.35 to

0.75 V (3 cycles) at  $100 \text{ mV}\cdot\text{s}^{-1}$ , galvanostatic electrodeposition at  $300 \text{ }\mu\text{A}\cdot\text{cm}^{-2}$  (normalized to the geometric electrode area) was performed to final deposited charges,  $Q_c$ , of 25 to  $100 \text{ mC}\cdot\text{cm}^{-2}$  (see Fig. S1 for a typical set of electrochemical data). The as-prepared  $\text{MnO}_2$ -GLAD-ITO electrodes were next carefully rinsed with milliQ water and soaked 30 min in 1 M KCl aqueous solution to remove all traces of electrolyte prior to galvanostatic cycling. The modified electrodes' homogeneous brown color (see Fig. S2) is characteristic of uniform  $\text{MnO}_2$  electrodeposition. We previously established that the quantity of electrodeposited  $\text{MnO}_2$  (in  $\text{mg}\cdot\text{cm}^{-2}$ , normalized to the geometric electrode area) scales linearly with the deposited charge  $Q_c$  (in  $\text{C}\cdot\text{cm}^{-2}$ ) according to the following relationship:<sup>[2]</sup>

$$m_{\text{MnO}_2} = (0.484 \pm 0.008) \times Q_c$$

**Preparation of the “MnO-based electrolyte”.** 7.1 mg/mL of MnO was added to a 2 m Al(OTf)<sub>3</sub> electrolyte and left for a few hours. The solution was then filtered to remove undissolved MnO. The filtrate of pH 1.6 was slightly yellow and it was then directly used with a fresh GLAD-ITO electrode for galvanostatic cycling.

**Spectroelectrochemistry.** Spectroelectrochemical experiments were performed in a quartz UV-visible cell modified to accommodate three electrodes with an electrolyte volume of 1.2 mL. The counter electrode was a Pt grid (0.06 mm wire diameter, 0.25 mm nominal space, Goodfellow) or a zinc foil (0.35 mm thickness, Goodfellow) and the reference electrode was a Dri-Ref Ag/AgCl/KCl<sub>sat</sub> electrode (+0.2 V vs. NHE, WPI Instruments). Unless otherwise stated, all reported potentials are quoted against this reference electrode. The UV-visible absorption spectra were recorded in transmission mode using an HR-2000+ spectrometer (Ocean Optics) controlled by the SpectraSuite software. Spectra were obtained by averaging 50 individual spectra recorded with an integration time of 40 ms.

**Zn/MnO<sub>2</sub> battery cell configuration.** The cyclability of the Zn/MnO<sub>2</sub> cell assemblies (2-electrode configuration) was investigated in a glass cell containing a  $\text{MnO}_2$ -GLAD-ITO electrode as the cathode, a zinc foil (0.35 mm thickness, Goodfellow) as the anode (electroactive surface area of  $0.5 \pm 0.1 \text{ cm}^2$  delimited by nail varnish), and 5 mL of aqueous electrolyte. The electrochemical cell was sealed with a septum to avoid evaporation of the aqueous electrolyte over long-term cycling (see Fig. S4). Cycles were performed by fixing the charge to  $0.1 \text{ C}\cdot\text{cm}^{-2}$  and the discharge cut-off value to 0.5 V. The first discharges were

performed at  $0.3 \text{ mA}\cdot\text{cm}^{-2}$ , while the subsequent charge/discharge cycles were performed at  $0.5 \text{ mA}\cdot\text{cm}^{-2}$ .

**Swagelok Zn/MnO<sub>2</sub> battery cell configuration.** Self-standing electrospun carbon nanofibers were prepared as described previously,<sup>[3]</sup> and used as cathode material in a swagelok cell (12 mm diameter PTFE cell with glassy carbon current collectors). The CNF loading was  $2.22 \text{ mg}\cdot\text{cm}^{-2}$  (corresponding to a thickness of  $360 \text{ }\mu\text{m}$ ), and the surface exposed to the electrolyte was  $0.785 \text{ cm}^2$ . A zinc foil (0.35 mm thickness, Goodfellow) of same surface was used as the anode, and the swagelok cell was filled with  $800 \text{ }\mu\text{L}$  of the aqueous electrolyte. Next, the following protocol was used: (i) *in-situ* MnO<sub>2</sub> electrodeposition up to  $1 \text{ C}\cdot\text{cm}^{-2}$  from the 1 M acetate buffer (pH 5) containing 0.1 M MnCl<sub>2</sub> and 0.85 M KCl at  $1 \text{ mA}\cdot\text{cm}^{-2}$ ; (ii) rinsing of the cell by a succession of water withdrawals/additions and then of the final electrolyte (1.3 m Al(OTf)<sub>3</sub> + 0.3 m Zn(OTf)<sub>2</sub> + 0.3 m MnCl<sub>2</sub>, pH 1.74) ; (iii) first discharge at  $0.63 \text{ mA}\cdot\text{cm}^{-2}$  ; (iv) following charge (up to  $1 \text{ C}\cdot\text{cm}^{-2}$ )/discharge cycles at  $1 \text{ mA}\cdot\text{cm}^{-2}$ .

**Galvanostatic experiments.** The (spectro)electrochemical cell was controlled by a VSP BioLogic potentiostat interfaced with EC-Lab 11.3 software. During the galvanostatic cycling experiments, a period of 30 s at the open circuit potential was systematically added at the end of each charge and discharge step to allow for relaxation of the potential. For GLAD-ITO electrodes, the charge was fixed to  $100 \text{ mC}\cdot\text{cm}^{-2}$ , with a duration cut-off of 200 s at  $0.5 \text{ mA}\cdot\text{cm}^{-2}$ . The charge and discharge cut-off potentials were fixed for the spectroelectrochemical experiments at +1.2 and +0.15 V *vs.* the Ag/AgCl reference electrode, and for cell assemblies at +2.5 and +0.5 V *vs.* the Zn counter electrode.

All gravimetric intensities ( $\text{A}\cdot\text{g}^{-1}$ ) were calculated from the current density ( $\text{mA}\cdot\text{cm}^{-2}$ ) applied to the electrode and the mass of MnO<sub>2</sub> electrodeposited *ex situ* ( $48.4 \text{ }\mu\text{g}\cdot\text{cm}^{-2}$ ). The Coulombic efficiency (*CE*), energetic efficiency (*EE*), and gravimetric capacity (*C<sub>g</sub>* in  $\text{mA}\cdot\text{h}\cdot\text{g}^{-1}$ ) were calculated using the following equations:

$$CE = \frac{Q_{i,disch}}{Q_{i,ch}} ; \quad EE = \frac{E_{i,disch}}{E_{i,ch}} ; \quad C_g = \frac{1000}{3.6} \frac{Q_{i,disch}}{0.484}$$

where  $Q_{i,ch}$  and  $Q_{i,disch}$  are the areal charging and discharging capacities of the *i*-th cycle in  $\text{mC}\cdot\text{cm}^{-2}$ , and  $E_{i,ch}$  and  $E_{i,disch}$  the corresponding charging and discharging energy densities in  $\text{W}\cdot\text{h}\cdot\text{cm}^{-2}$  determined from the product of *Q* and the average charge/discharge voltages.

**X-Ray fluorescence spectrometry (XRF).** After cycling, the electrodes were soaked in milliQ water for a few minutes to remove the electrolyte and then left to dry at ambient temperature prior to analysis. A Panalytical Epsilon 3XL spectrometer, equipped with an Ag X-ray tube and operating under an He atmosphere, was used under 3 conditions, *i.e.* 50 kV–6  $\mu$ A for 180 s to analyze In and Sn, 20kV–15  $\mu$ A for 60 s to analyze Mn, and 5 kV–60  $\mu$ A for 60 s to analyze Al. Calibrations were established by analyzing 1 g/L certified solutions of the 4 elements (Inorganic Ventures), and using exactly the same measurement conditions. For aluminium, the limit of detection and limit of quantification were 47 and 156 ng, respectively, while for manganese, they were 17.5 ng and 58.5 ng, respectively.

In order to ensure equivalent surface area analysis for all samples, a delimited area of 0.16 cm<sup>2</sup> located within the electroactive surface area of the electrode was exposed to the X-Ray beam (through a steel mask). We noticed that a small amount of Mn was detected in bare GLAD-ITO electrodes, most likely arising from the commercial ITO-glass substrate. In all samples analyzed, the amount of Al detected was below the limit of quantification. For the electrodes loaded *ex situ*, a linear relationship was obtained between the *ex situ* charge  $Q_c$  of the electrode and the areal mass of Mn quantified by XRF (see Fig. S3). This confirms that XRF provides quantitative analysis of the Mn mass remaining over the surface of cycled GLAD-ITO electrodes. However, the  $m_{\text{Mn}}$  (in  $\mu\text{g}\cdot\text{cm}^{-2}$ ) deduced from XRF was systematically lower than that determined by ICP quantification, which is most likely due to uncertainties in both the exact surface exposed (notably because of the incidence angle of the X-Ray beam) as well as matrix effects. Therefore, the ICP data were used as a reference to adjust the XRF calibration plot in Fig. S3, leading to a correcting factor 1.347. The  $m_{\text{MnO}_2}$  (in  $\mu\text{g}\cdot\text{cm}^{-2}$ ) was finally calculated from  $m_{\text{Mn}}$  as determined by XRF according to the following equation:

$$m_{\text{MnO}_2} = \frac{87}{55} \times 1.347 \times (m_{\text{Mn}} - 1.91)$$

## II. Supplementary Figures

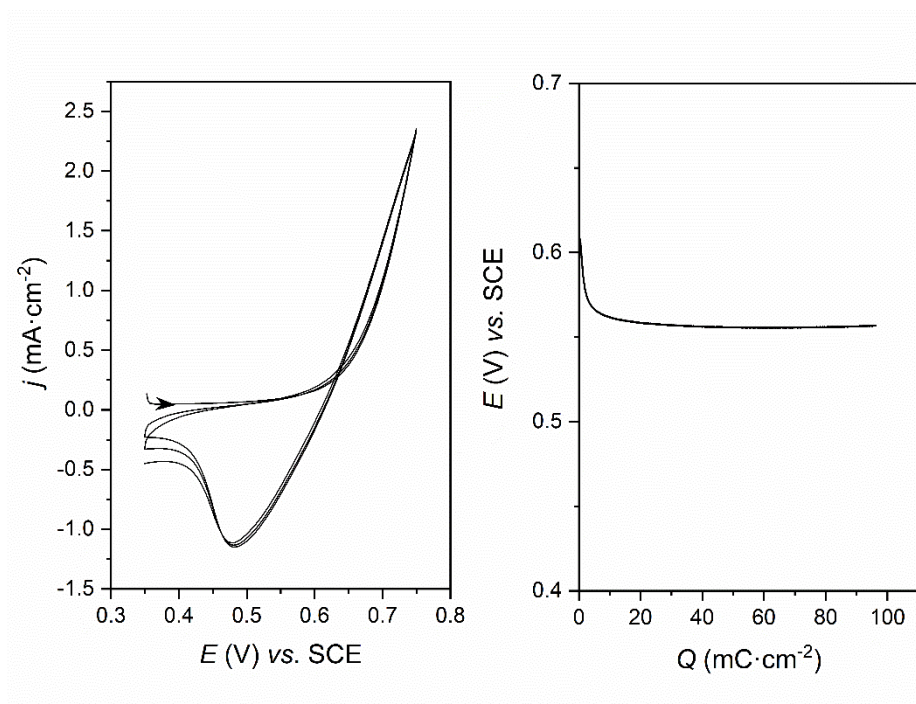


**Figure S1.** *Ex situ* electrochemical loading of the GLAD-ITO electrodes through successive (left) cyclic voltammograms at 100 mV·s<sup>-1</sup> followed (right) by a galvanostatic charge at 0.3 mA·cm<sup>-2</sup>.

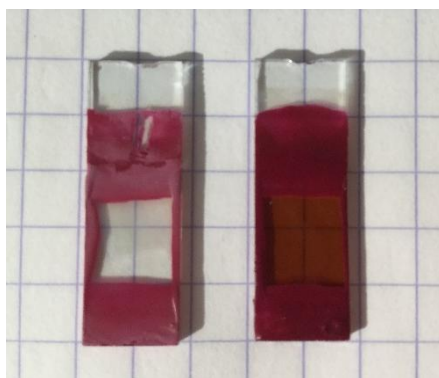


**Figure S2.** Photograph of the GLAD-ITO electrode (left) before and (right) after *ex situ* loading to 100 mC·cm<sup>-2</sup>.

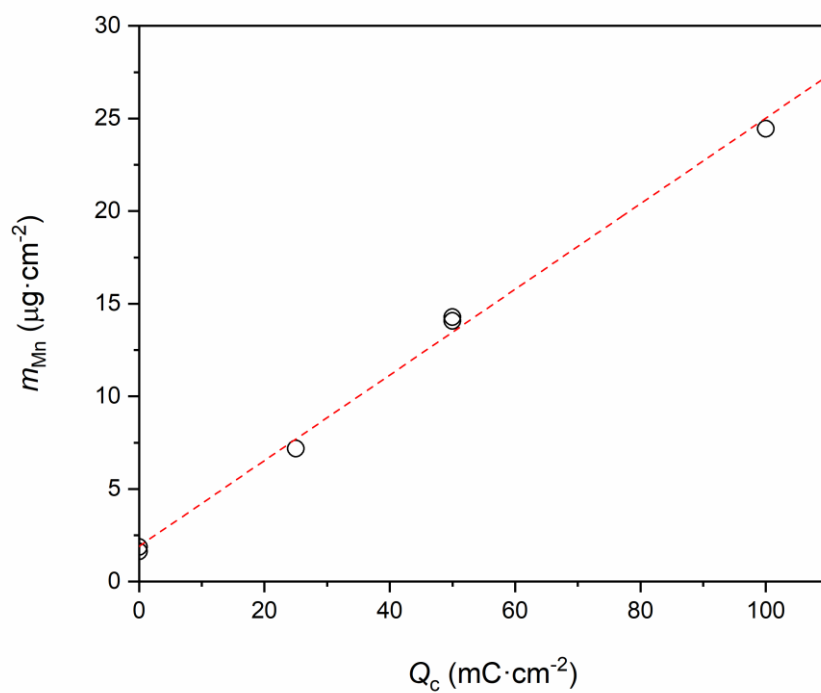


**Figure S3.** Linear relationship between the areal mass of Mn determined by XRF (normalized to the exposed geometric surface area) and the *ex situ* loading charge  $Q_c$ . The experimental data were fitted to a linear regression with a slope of 0.23, an intercept at 1.91, and a  $R^2$  value of 0.995.

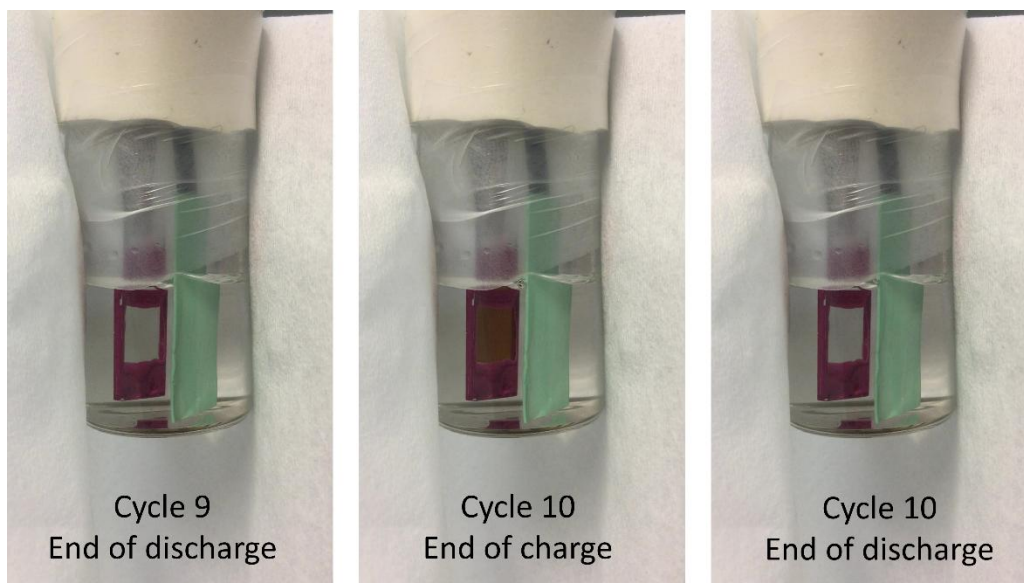


**Figure S4.** Photographs taken during the 10<sup>th</sup> galvanostatic cycle recorded at a Zn/MnO<sub>2</sub>-GLAD-ITO assembly. Electrolyte: 1.25 M Al(OTf)<sub>3</sub>, 0.1 M ZnCl<sub>2</sub>, 0.1 M MnCl<sub>2</sub> (pH 1.5).

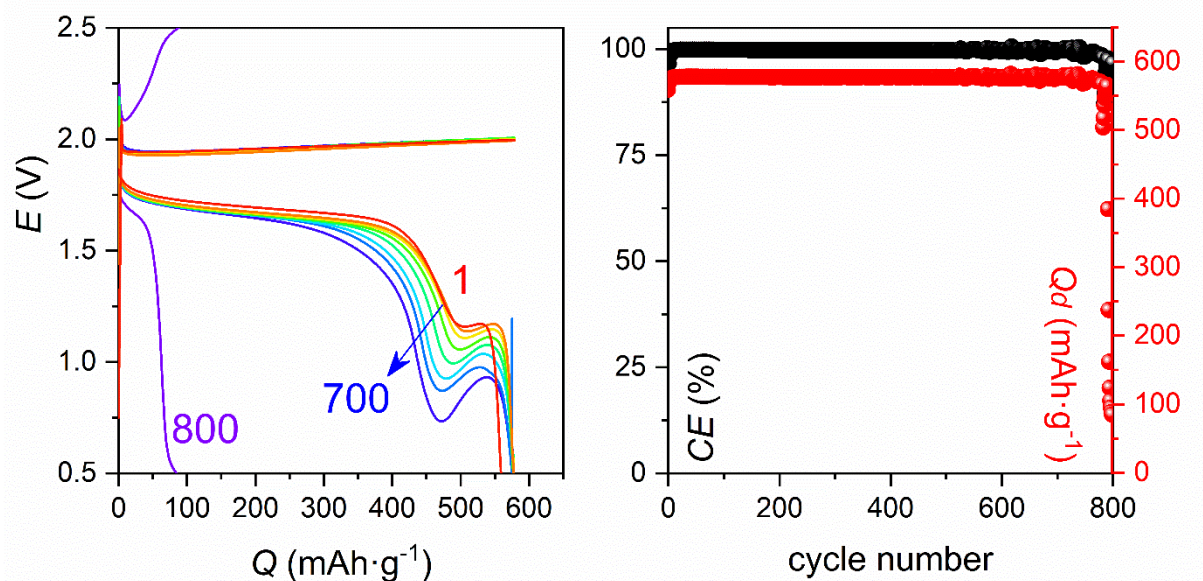


**Figure S5.** Long-term cycling of the Zn/MnO<sub>2</sub>-GLAD-ITO assembly in 1 m Al(OTf)<sub>3</sub> + 1 m Zn(OTf)<sub>2</sub> + 0.1 m MnSO<sub>4</sub> (pH 1.75) solution at a rate of 10 A·g<sup>-1</sup>.

**Comment.** During long term cycling, the Zn/MnO<sub>2</sub>-GLAD-ITO cell shows a progressive evolution of the shape of the discharge curve in contrast to the charge curve which overlaps perfectly. Then from the 780 cycle, a sudden loss of the cell charging capacity is noted over a few cycles, signalling the shutdown of the cell. For the moment, we have no explanation for this behaviour.

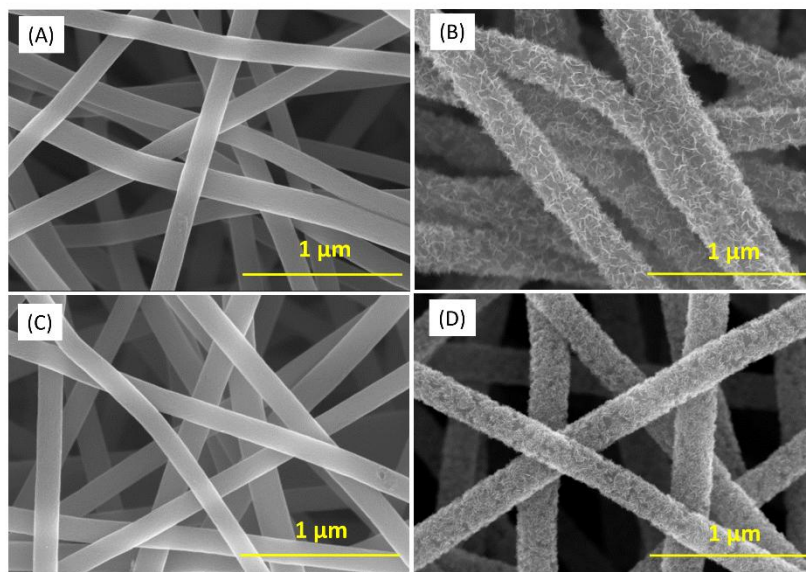


**Figure S6.** SEM images of the CNF cathode at different stages of the cycling protocol used in this study, starting from (A) pristine CNF cathode. (B)  $\text{MnO}_2$ -loaded cathode after  $\text{MnO}_2$ -electrodeposition ( $1 \text{ C}\cdot\text{cm}^{-2}$ ) at  $1 \text{ mA}\cdot\text{cm}^{-2}$ . (C) Cathode after 1<sup>st</sup> discharge in  $1.3 \text{ m Al(OTf)}_3 + 0.3 \text{ m Zn(OTf)}_2 + 0.3 \text{ m MnCl}_2$  (pH 1.74) aqueous electrolyte at  $0.63 \text{ mA}\cdot\text{cm}^{-2}$ . (D) Cathode after following charge ( $1 \text{ C}\cdot\text{cm}^{-2}$ ) in the same  $\text{Al}^{3+}$ -based electrolyte at  $1 \text{ mA}\cdot\text{cm}^{-2}$ .

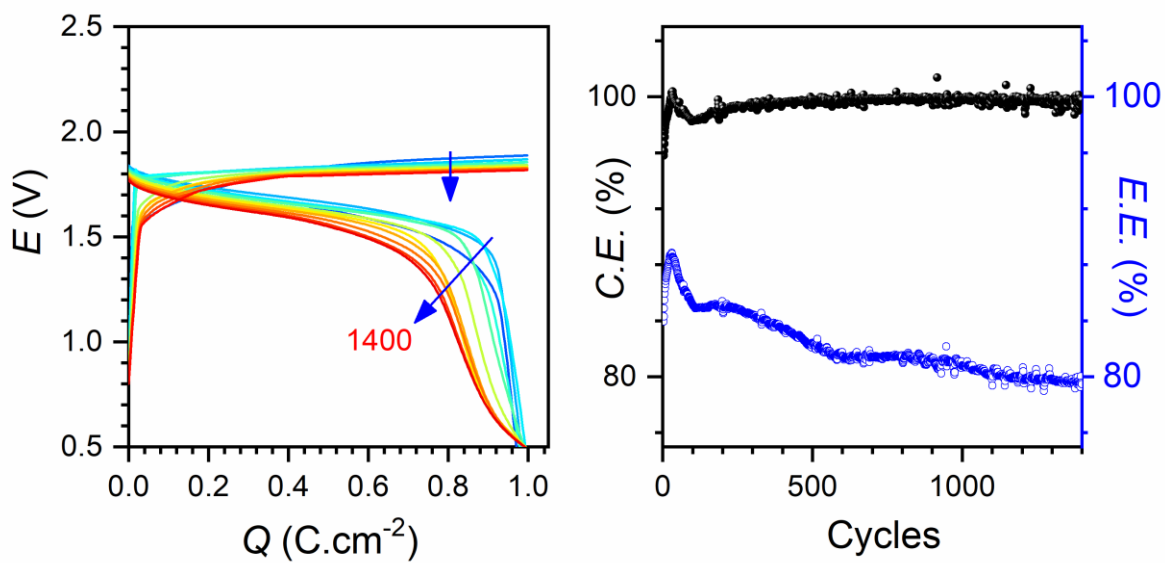


**Figure S7.** Long-term cycling of the Zn/MnO<sub>2</sub> Swagelok assembly in 1.3 m Al(OTf)<sub>3</sub> + 0.3 m Zn(OTf)<sub>2</sub> + 0.3 m MnCl<sub>2</sub> (pH 1.74) solution at a rate of 2 A·g<sup>-1</sup>. From blue to red: cycle number 10, 50, 100, 200, 400, 600, 1000, 1200, 1400.

### III. Supplementary Tables

**Table S1.** Chemical composition of the aqueous electrolytes used for the spectroelectrochemical experiments and main features (potential, charge, absorbance and mass of Mn) of the *ex situ* galvanostatic charges and first *in situ* galvanostatic discharges.

	Electrolyte composition	pH	$E_c$ (V vs. Ag/AgCl)	$Q_c$ (mC·cm <sup>-2</sup> )	$\Delta A$ at end of the charge or of the 1 <sup>st</sup> discharge	$m_{\text{MnO}_2}$ (μg·cm <sup>-2</sup> ) at end of the charge or of the 1 <sup>st</sup> discharge
<i>Ex situ</i> galvanostatic charge	1 M acetate buffer + 0.1 M MnCl <sub>2</sub> + 0.85 M KCl	5.0	0.600	100	0.86 ± 0.03	48
1 <sup>st</sup> <i>in situ</i> galvanostatic discharge	1 M AlCl <sub>3</sub> + 0.1 M MnCl <sub>2</sub>	2.10	0.767	97	0.01	-
	1 M Al(OTf) <sub>3</sub> + 0.1 M MnCl <sub>2</sub>	1.98	0.750	96	0.02	0.3
	1 M acetic acid + 0.1 M MnCl <sub>2</sub> + 2 M KCl	2.05	0.742	92	0.04	1.9
	2 M KCl + 0.1 M MnCl <sub>2</sub> + acidified with 3 M HCl	2.05	0.415	43	0.33	28
	2 M KCl + 0.1 M MnCl <sub>2</sub> + acidified with 3M HCl	1.0	0.975	99	0.004	-

**Table S2.** Concentration, molality and pH of aqueous electrolytes prepared from various  $\text{Al}^{3+}$ - or  $\text{Zn}^{2+}$ - inorganic in milliQ water.

Salt	$\text{Al}^{3+}$ or $\text{Zn}^{2+}$ <sup>a, b</sup>	$\text{Al}^{3+}$ or $\text{Zn}^{2+}$ <sup>a, b</sup>	pH
	Concentration (M in mol/L)	molality (m in mol/kg)	
$\text{Al}(\text{OTf})_3$	2	3.7	< 0
	<i>1.4</i>	2	1.4
	1	<i>1.3</i>	2.05
Anhydrous $\text{AlCl}_3$	2	<i>2.1</i>	0.85
	1		2.2
$\text{Zn}(\text{OTf})_2$	2	<i>2.7</i>	3.8
	<i>1.7</i>	2	4.35
$\text{Al}(\text{OTf})_3 + \text{Zn}(\text{OTf})_2$	1 each		0.7
		1 each	1.75

<sup>a</sup> Solutions were prepared in a volumetric flask, to avoid volumetric issues associated to the high mass of salt required for concentrations in the molar range.

<sup>b</sup> Italic values were calculated from experimental data (*i.e.*, from mass of water added in the volumetric flask for electrolytes prepared in molarity or from final volume of the mixture for electrolytes prepared in molality)

**Comment on the electrolyte preparation.** Preparing aqueous electrolytes with inorganic salts at a molar concentration requires taking into account the volume occupied by the large amount of inorganic salt. This is especially true with triflate salts, which have very low density. We notice that this is not done in some publications mentioning molarities for electrolytes prepared from mixing a certain mass of the inorganic salt with a fixed volume of water without considering the volume expansion.<sup>[4–6]</sup>

As an illustration, we prepared a “2 M  $\text{Al}(\text{OTf})_3$ ” aqueous electrolyte by mixing 10 mmol of  $\text{Al}(\text{OTf})_3$  (4.74 g of the dry corresponding salt occupying a volume of ca. 4 mL) with 5 mL milliQ water. After complete dissolution of the inorganic salt, the final volume of the solution was 7.2 mL and its final mass was 9.72 g. Accordingly, the real concentration of the electrolyte is  $1.4 \text{ mol}\cdot\text{L}^{-1}$  (instead of 2 M). We also measured the pH after the solution was left to recover ambient temperature (since dissolution is exothermic) and a value of 1.4 was determined.

**Table S3.** Main chemical and electrochemical features of the Zn/MnO<sub>2</sub>-GLAD-ITO cell assemblies. *CE* and *EE* are average values over 100 cycles.

Electrolyte composition	pH	$E_d$ (V)	$\Delta E^a$ (V)	$CE \pm 3\sigma^b$ (%)	$EE \pm 3\sigma^b$ (%)
1 M AlCl <sub>3</sub> , 0.25 M ZnCl <sub>2</sub> , 0.1 M MnCl <sub>2</sub>	1.9	1.76	0.24	99.3 $\pm$ 0.2	83.1 $\pm$ 1.8
1 M Al(OTf) <sub>3</sub> , 0.1 M ZnCl <sub>2</sub> , 0.1 M MnCl <sub>2</sub>	1.77	1.65	0.25	98.6 $\pm$ 0.3	80.3 $\pm$ 1.5
1.25 M Al(OTf) <sub>3</sub> , 0.1 M ZnCl <sub>2</sub> , 0.1 M MnCl <sub>2</sub>	1.5	1.70	0.29	99.6 $\pm$ 0.2	81.3 $\pm$ 2.8
1 m Al(OTf) <sub>3</sub> , 1 m Zn(OTf) <sub>3</sub> , 0.1 m MnSO <sub>4</sub>	1.75	1.67	0.30	99.7 $\pm$ 1.2	80.0 $\pm$ 1.7

<sup>a</sup> Voltage hysteresis

<sup>b</sup>  $\sigma$  is the standard deviation

**Comment on the bi-cation electrolyte.** With the cycling of the Zn/MnO<sub>2</sub>-GLAD-ITO assembly in an electrolyte containing 1 m Al(OTf)<sub>3</sub>, 1 m ZnCl<sub>2</sub>, and 0.1 m MnSO<sub>4</sub> at pH 1.4, we demonstrate that MnO<sub>2</sub>-to-Mn<sup>2+</sup> conversion is the main charge storage mechanism occurring at the cathode in such electrolyte. The corresponding charge/discharge potentials as well as potential hysteresis are very close to those reported for a Zn/ $\alpha$ -MnO<sub>2</sub> assembly cycled in a (1 M Al(OTf)<sub>3</sub>, 1 M Zn(OTf)<sub>2</sub>, 0.1 M MnSO<sub>4</sub>) bi-cation electrolyte (see Table 1).<sup>[4]</sup> This result strongly supports a unified charge storage mechanism in both electrolytes. It is worth noting here that our attempts at dissolving 0.1 M MnSO<sub>4</sub> in a 1 M Al(OTf)<sub>3</sub> and 1 M Zn(OTf)<sub>2</sub> mixture were unsuccessful, which brings us to assume that the authors refer rather to molality than molarity (see comment below Table S2 on the electrolyte composition) and thus that the electrolyte compositions are in fact identical in both studies. Furthermore, we also demonstrate that similar electrochemical features are retrieved in an electrolyte made of a mixture of 1.25 M Al(OTf)<sub>3</sub>, 0.1 M ZnCl<sub>2</sub>, and 0.1 M MnCl<sub>2</sub> at a same pH (see Table 1). Thus, replacing most of the Zn<sup>2+</sup> ions with Al<sup>3+</sup> ions does not affect the electrochemical features of the Zn/MnO<sub>2</sub> assembly, which is fully consistent with a cathode charge storage mechanism that does not rely on the reversible insertion of Zn<sup>2+</sup> ions. Besides, the conversion mechanism allows us to rationalize the significant up-shift of the charge/discharge potentials (+ 0.26 V) reported by the authors upon switching from a 2 m Zn(OTf)<sub>2</sub> electrolyte to a mixture of 1 m Al(OTf)<sub>3</sub> and 1 m Zn(OTf)<sub>2</sub>. Indeed, this is associated with a significant acidification of the electrolyte (we estimate a  $\Delta$ pH value of -2.6 based on the data of Table S3). On account of the pH-independence of the Zn<sup>2+</sup>-to-Zn electrochemical reaction and the pH-dependence of the MnO<sub>2</sub>-to-Mn<sup>2+</sup> conversion reaction within the pH range investigated, the +0.26 V up-shift translates into a pH decrease of 2.2, which is close to the  $\Delta$ pH value between the mono-cation and the bi-cation electrolytes.

#### IV. References

- [1] K. M. Krause, M. T. Taschuk, K. D. Harris, D. A. Rider, N. G. Wakefield, J. C. Sit, J. M. Buriak, M. Thommes, M. J. Brett, *Langmuir* **2010**, *26*, 4368.
- [2] M. Mateos, K. D. Harris, B. Limoges, V. Balland, *ACS Appl. Energy Mater.* **2020**, *3*, 7610.
- [3] A. Singh, O. Sel, H. Perrot, V. Balland, B. Limoges, C. Laberty-Robert, *J. Mater. Chem. A* **2021**, Advance Article.
- [4] N. Li, G. Li, C. Li, H. Yang, G. Qin, X. Sun, F. Li, H. Cheng, *ACS Appl. Mater. Interfaces* **2020**, *12*, 13790.
- [5] C. Yan, C. Lv, L. Wang, W. Cui, L. Zhang, K. N. Dinh, H. Tan, C. Wu, T. Wu, Y. Ren, J. Chen, Z. Liu, M. Srinivasan, X. Rui, *J. Am. Chem. Soc.* **2020**, *142*, 15295615304.
- [6] S. He, J. Wang, X. Zhang, J. Chen, Z. Wang, T. Yang, Z. Liu, Y. Liang, B. Wang, S. Liu, L. Zhang, J. Huang, J. Huang, L. A. O. Dell, H. Yu, *Adv. Funct. Mater.* **2019**, 1905228.